Organic & Biomolecular Chemistry

ROYAL SOCIETY OF CHEMISTRY

PAPER

View Article Online
View Journal | View Issue

Cite this: *Org. Biomol. Chem.*, 2025, **23**, 3619

Construction of multi-functionalized carbon chains by Ni-catalyzed carbosulfonylation of butadiene†

Yan Liu,[a,b] Xiang-Xin Zhang,[a,b] Xue-Ting Li,[a,b] Su-Yang Xu,[a,b] Ding-Wei Ji[a] and Qing-An Chen*[a,b]

Received 5th March 2025,
Accepted 13th March 2025

DOI: 10.1039/d5ob00402k

rsc.li/obc

Multi-functionalized carbon chains are prevalent motifs existing in various natural products and drugs. How to construct multi-functionalized carbon chains represents a meaningful task. Herein, we developed a photo-induced stereoselective 1,4-carbosulfonylation of butadiene to construct multi-functionalized carbon chains under nickel catalysis. A wide variety of aryl iodides and sodium sulfinates could be facilely coupled with butadiene to generate difunctionalized olefin intermediates. Taking advantage of the internal C=C bond, various functional groups have been efficiently incorporated to construct multi-functionalized aliphatic compounds. A scale-up reaction, an iterative reaction and late-stage modifications have been performed to further demonstrate the synthetic utility of this protocol.

Multi-functionalized aliphatic moieties are widely found in a variety of natural products, such as glucose, ribose, and tartaric acid, with multiple hydroxyl functional groups.[1] In addition, multi-functionalized molecules are important structural components in pharmaceuticals, such as paclobutrazol,[2] amprenavir,[3] bestatin,[4] and atazanavir[5] (Fig. 1A). Conventional methods to access these valuable structures need well-designed multi-step syntheses which also suffer from time and economic issues. In recent years, C–H bond activation has emerged as a powerful strategy for molecular functionalizations.[6] It provides an ideal approach for the construction of mono-functionalized carbon chains (Fig. 1B). In contrast, only limited progress has been made in multiple C–H bond activation. For example, Lambert and co-workers reported the conversion of unactivated vicinal C–H bonds to C–N bonds[7] or C–O bonds[8] to form 1,2-difunctionalization derivatives through an electrophotocatalytic strategy. However, it is difficult to rapidly construct those multi-functionalized molecules in this way because of synthetic challenges on the control of chemo-, regio- and stereoselectivities. Meanwhile, it will generate a huge amount of waste. Thus, developing a novel and divergent method for the construction of multi-functionalized carbon chains is highly desirable.

Recently, the merger of visible light photocatalysis and transition metal catalysis has emerged as a powerful tool in organic synthesis.[9] In particular, the combination of nickel catalysis and photocatalysis has evolved into an attractive protocol in homogeneous catalysis.[10] Being considered as a bioisostere[11] of the carbonyl group, sulfinates have been used as radical precursors to construct sulfones under photocatalysis.[12] Notably, significant progress has been achieved in the carbosulfonylation of conventional alkenes and alkynes by Rueping, Lu, Nevado and Chu.[13] Only one example of carbosulfonylation has been reported using 2,3-dimethyl-1,3-butadiene as a conjugated diene and poor stereoselectivity (1.3/1) was observed.[13a] Yang's group demonstrated a photoinduced 1,2-alkylsulfonylation of aryl dienes under Pd catalysis (Fig. 1C).[13i] However, the construction of more challenging multi-functionalized carbon chains remained underdeveloped. Inspired by these precedents and our continued interest in photocatalysis[14] and diene functionalization,[15] we herein developed a photo-induced stereoselective 1,4-carbosulfonylation of butadiene to construct multi-functionalized carbon chains under nickel catalysis (Fig. 1D). Our protocol provides an expedient approach for the construction of multi-functionalized complex scaffolds.

The optimization of the reaction conditions is briefly summarized in Table 1. Initially, iodobenzene (**1a**), butadiene (**2a**) and sodium benzenesulfinate (**3a**) were selected as the model substrates to investigate the reaction conditions in the presence of 4CzIPN, $NiBr_2$ and 1,10-phenanthroline (**L1**). The

[a]*Dalian Institute of Chemical Physics, Chinese Academy of Sciences, Dalian 116023, People's Republic of China. E-mail: qachen@dicp.ac.cn*
[b]*University of Chinese Academy of Sciences, Beijing 100049, People's Republic of China*

†Electronic supplementary information (ESI) available. CCDC 2335639, 2369001 and 2369003. For ESI and crystallographic data in CIF or other electronic format see DOI: https://doi.org/10.1039/d5ob00402k

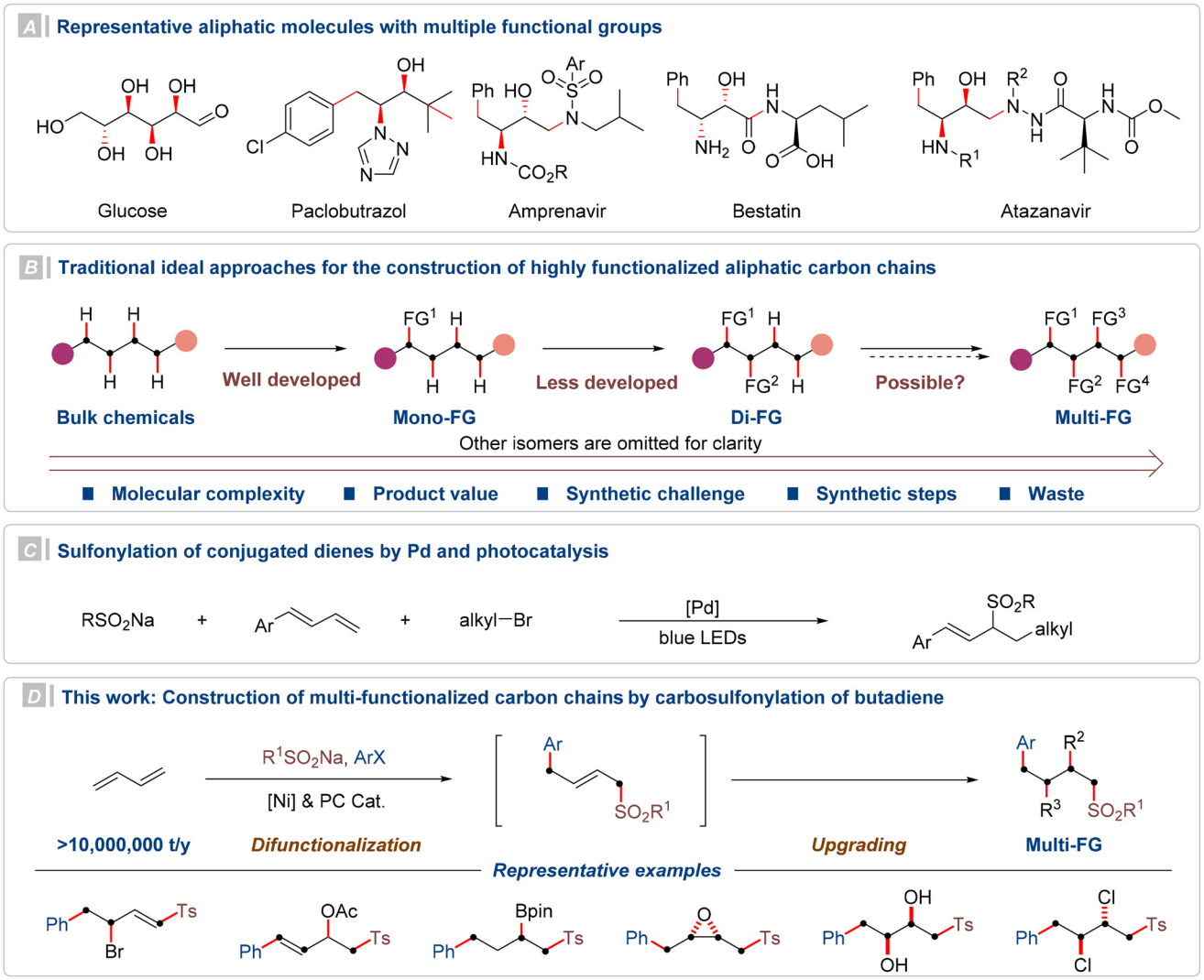

Fig. 1 Representative highly functionalized aliphatic molecules and strategies of construction.

desired product **4aa** was formed in 69% yield with good stereoselectivity (entry 1). The dimethyl-substituted phenanthroline ligand sharply decreased the reaction efficiency (please see the ESI† for details). Besides, other nitrogen ligands with distinct backbones were also tested, and terpyridine (**L2**) afforded **4aa** in only 3% yield (entry 2). It is worthwhile to mention that bidentate nitrogen ligands 2,2′-bipyridine (bpy) **L3** could promote the process with 88% yield (entry 3). Compared with 4CzIPN, $[Ir(ppy)_2(dtbbpy)]PF_6$ showed a better catalytic effect with 91% yield (entry 4). A series of dipyridyl bridging ligands possessing various substituents were further examined (entries 5–9). The 4,4′-CO_2Me bpy ligand (**L8**) had an intriguing effect on the *E*/*Z* selectivity, although it resulted in a decreased yield (entry 9). Further evaluation of nickel catalysts disclosed (entries 10–12) that $NiBr_2$·DME was the most suitable catalyst, giving **4aa** in 84% yield with up to 20/1 *E*/*Z* selectivity (entry 12). Finally, control experiments showed that no target product was formed under the conditions without a photocatalyst, a nickel catalyst or blue light. Only a trace amount of the target product could be detected without the ligand (entries 13–16).

With the optimized reaction conditions in hand, the scope of sulfinates was investigated next (Fig. 2). Firstly, sodium benzenesulfinate (**3a**) without any substituent group on phenyl was treated under the standard conditions, which could deliver the target product **4aa** in 84% yield. The structure of **4aa** was confirmed by single-crystal X-ray diffraction (CCDC 2335639†). Sulfinates containing methoxyl, alkyl, and aryl at the *para*-position were good substrates for this reaction, affording **4ab**, **4ac** and **4ae** in 77–97% yields. Benzenesulfinate with 4-phenoxy was incorporated in the reaction to give **4ad** in 41% yield due to solubility issues. Introducing different electron-withdrawing groups such as F, Cl, Br, and CF_3 resulted in the formation of the corresponding sulfonylarylation products **4af–4ai** in moderate to good isolated yields (61–88%) with high stereoselectivities. *ortho*- and *meta*-Substituted sodium benzenesulfinates gave comparable yields (66–92%) and stereoselec-

Table 1 Optimization of the reaction conditions[a]

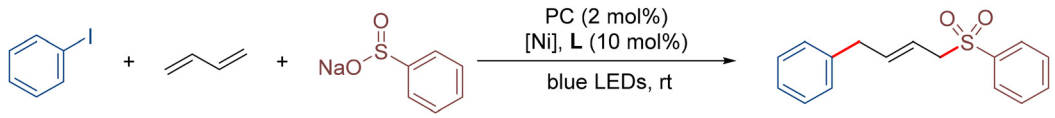

Entry	PC	[Ni]	Ligand	Yield (%)	*E*/*Z*
1	4CzIPN	$NiBr_2$	**L1**	69	13/1
2	4CzIPN	$NiBr_2$	**L2**	3	—
3	4CzIPN	$NiBr_2$	**L3**	88	13/1
4	$[Ir(ppy)_2(dtbbpy)]PF_6$	$NiBr_2$	**L3**	91	14/1
5	$[Ir(ppy)_2(dtbbpy)]PF_6$	$NiBr_2$	**L4**	35	11/1
6	$[Ir(ppy)_2(dtbbpy)]PF_6$	$NiBr_2$	**L5**	90	8/1
7	$[Ir(ppy)_2(dtbbpy)]PF_6$	$NiBr_2$	**L6**	90	10/1
8	$[Ir(ppy)_2(dtbbpy)]PF_6$	$NiBr_2$	**L7**	89	10/1
9	$[Ir(ppy)_2(dtbbpy)]PF_6$	$NiBr_2$	**L8**	66	16/1
10	$[Ir(ppy)_2(dtbbpy)]PF_6$	$NiCl_2$	**L8**	33	9/1
11	$[Ir(ppy)_2(dtbbpy)]PF_6$	$NiCl_2$·DME	**L8**	68	12/1
12[b]	$[Ir(ppy)_2(dtbbpy)]PF_6$	$NiBr_2$·DME	**L8**	84	20/1
13	—	$NiBr_2$·DME	**L8**	N.D.	—
14	$[Ir(ppy)_2(dtbbpy)]PF_6$	—	**L8**	N.D.	—
15	$[Ir(ppy)_2(dtbbpy)]PF_6$	$NiBr_2$·DME	—	Trace	—
16[c]	$[Ir(ppy)_2(dtbbpy)]PF_6$	$NiBr_2$·DME	**L8**	N.D.	—

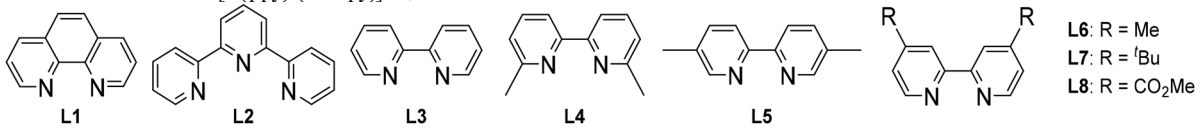

[a] Standard conditions: **1a** (0.20 mmol), **2a** (0.60 mmol), **3a** (0.40 mmol), PC (2 mol%), [Ni] (10 mol%), **L** (10 mol%), MeCN (1.8 mL), DMSO (0.2 mL), blue LEDs, 18 h, under N_2. Yields were determined by GC-FID analysis of the crude reaction mixture using mesitylene as an internal standard. [b] MeCN (1.0 mL), isolated yield. [c] In the dark.

tivities (**4aj–4am**). This protocol was also compatible with other aromatic groups, such as naphthyl (**4an**), thienyl (**4ao**) and pyridyl (**4ap**). It is worth noting that thienyl substituted sulfinates afforded the desired product **4ao** in up to 95% yield. Besides, alkyl sulfinates also worked well in the three-component cross-coupling reaction, affording acceptable yields (**4aq–4as**, 43–79%).

Subsequently, the generality of the multicomponent cross-coupling with regard to the electrophilic coupling partner was examined. As shown in Fig. 3, a variety of (hetero)aryl iodides performed well in this cross-coupling. The target product **4ba** could be obtained in 91% yield with up to 20/1 *E*/*Z* selectivity by using sodium 4-methylbenzenesulfinate (**3y**) as the model substrate. Functional groups including ketone and amide at the *ortho* position on phenyl were well tolerated, furnishing the corresponding carbosulfonylated products **4bb–4bc** in 99% and 80% yields, respectively. A series of substrates bearing halogens and trifluoromethyl at different positions of the benzene ring were employed and gave the corresponding products **4bd–4bg** and **4bj–4bm** in moderate to good yields (45–99%) and with excellent stereoselectivities. Next, electron-deficient aryl iodides with cyanide, ketone, and ester at the *para* position on phenyl (**4bn** and **4bp–4bq**) also served as effective coupling partners, resulting in high yields (77–99%). Moreover, several electron-rich and electron-neutral arenes containing methoxyl, tertiary butyl, phenyl, and naphthyl (**4bh–4bi**, **4bo**, and **4br**) were amenable for this coupling protocol (54–92% yields). Interestingly, heteroaryl iodides bearing benzo[*d*][1,3]dioxole, thiophene, pyridine and pyrazine moieties (**4bs–4bx**) were successfully applied in this synergistic protocol (25–99% yields). Notably, the method worked efficiently for *para*-substituted iodopyridine with 99% isolated yield (**4bv**). It demonstrates that this protocol has great potential for constructing nitrogen-containing natural products and drugs.

To demonstrate the synthetic utility of this carbosulfonylation of butadiene, more structurally complex reaction partners featuring motifs commonly found in natural products and pharmaceutically active molecules were examined in this protocol (Fig. 4a). These derivatized aryl iodides from lithocholic acid, indomethacin, oxaprozin, diacetone-D-glucose, febuxostat and (1*S*)-(−)-camphanic acid were compatible with this strategy, affording good yields (**5a–5f**). To illustrate the application of the reaction, a scale-up reaction was performed at the 5 mmol scale with half the amount of photocatalyst, nickel catalyst and ligand, delivering 1.17 g of target product **4ba** in 82% yield with excellent stereoselectivity (*E*/*Z* > 20/1).

Due to the existence of a double bond in the carbosulfonylation product of butadiene, further transformations could construct multi-functionalized carbon chains that are usually difficult to create (Fig. 4b). Epoxidation of the carbosulfonylation product **4ba** was achieved in the presence of *m*-CPBA to form the corresponding epoxide **6a** in 93% yield with four

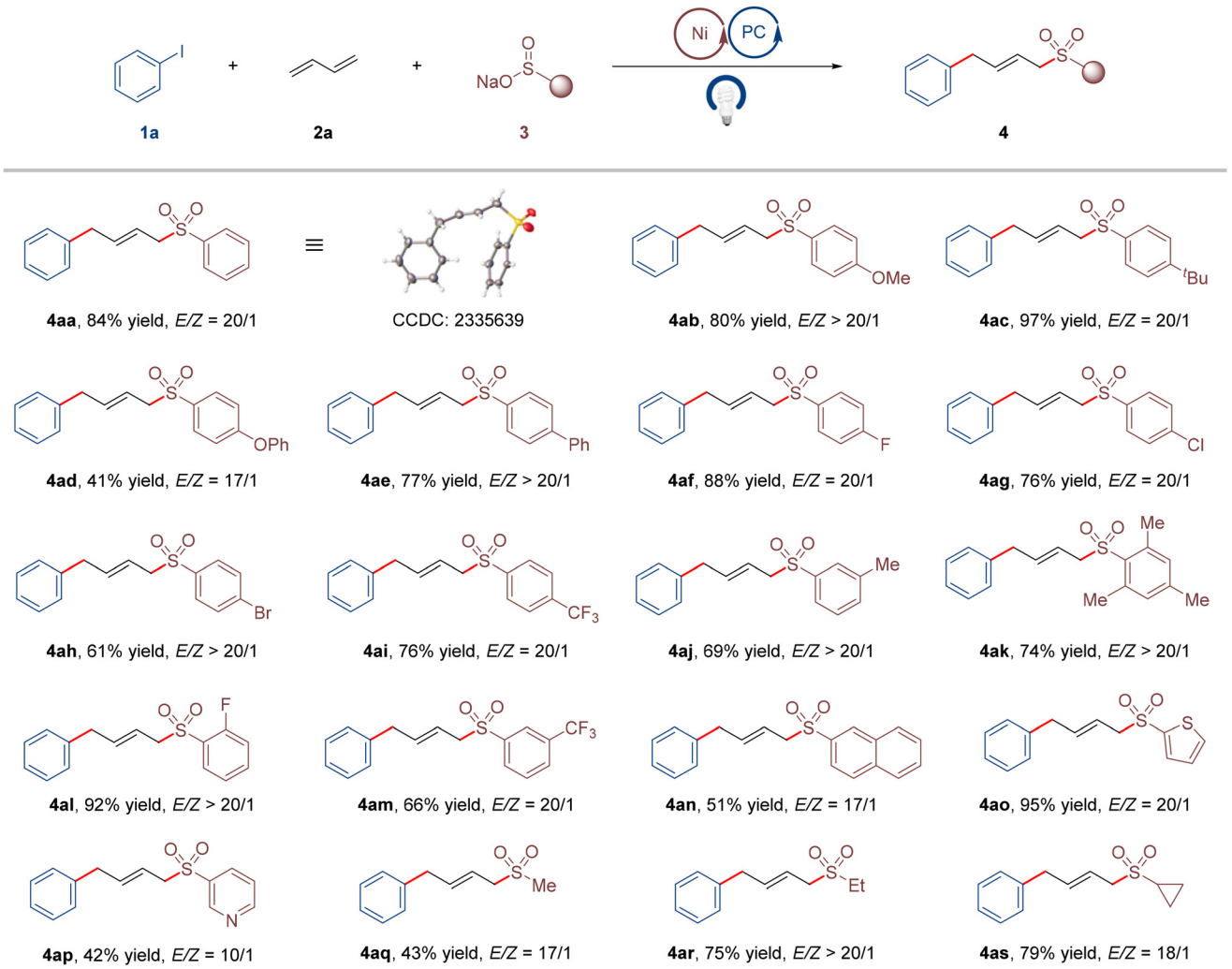

Fig. 2 Substrate scope of sulfinates. Conditions: **1a** (0.20 mmol), **2a** (0.60 mmol), **3** (0.40 mmol), $NiBr_2$·DME (10 mol%), $Ir(ppy)_2(dtbbpy)PF_6$ (2 mol%), **L8** (10 mol%), MeCN (1.0 mL), DMSO (0.2 mL), blue LEDs, 24 h, under N_2. Isolated yields are given.

functional groups. The carbosulfonylation product **4ba** could undergo hydroboration[16] and hydroxylation to give triple-functionalized carbon chains **6b** (53% yield) and **6c** (50% yield), respectively. Fortunately, subjecting **4ba** to osmium-catalyzed dihydroxylation afforded *syn*-diol **6d** in 82% yield with four functional groups. Next, the dichloride tetra-functional carbon chain product **6e** was obtained in *anti*-configuration. It is satisfactory that the products of double bond migration could be obtained, and different functional groups such as methoxy and bromine[17] groups could be installed simultaneously (**6f** and **6g**). Triple functional unsaturated carbon chains were obtained, which have the potential to install more functional groups. The structures of **6d** (CCDC 2369901†) and **6g** (CCDC 2369903†) were confirmed by single-crystal X-ray diffraction. To demonstrate the efficiency of the synthesis of multifunctionalized carbon chains, an iterative reaction was performed with 1,3-diiodobenzene (**1y**) and two different sodium sulfinates **3s** and **3o** under standard conditions in two steps, obtaining unsymmetrical product **7b** in 72% yield (Fig. 4c). To our delight, four hydroxyl groups could be installed at the same time to efficiently gain the highly functionalized carbon chain **7c** in 61% yield. The synthesis of multi-functionalized carbon chains provides an idea for the efficient synthesis of complex products with multi-functional groups that are difficult to synthesize by traditional methods or with complex synthesis steps.

In order to gain more insight into the mechanism of the metal-photoredox three-component-coupling protocol, some preliminary mechanistic experiments were conducted (Fig. 5). When the reaction mixture of iodobenzene (**1a**), butadiene (**2a**) and sodium benzenesulfinate (**3a**) was treated under the standard conditions in the presence of radical scavenger BHT, the yield of target product **4aa** was slightly inhibited. The desired reaction was suppressed when adding radical inhibitor TEMPO. This implies that a radical process is included in this protocol. The observation of BHT-adduct **8a** and TEMPO-adduct **8b** by ESI-HRMS suggests that a sulfonyl radical and the corresponding sulfonyl alkyl radical are likely produced in

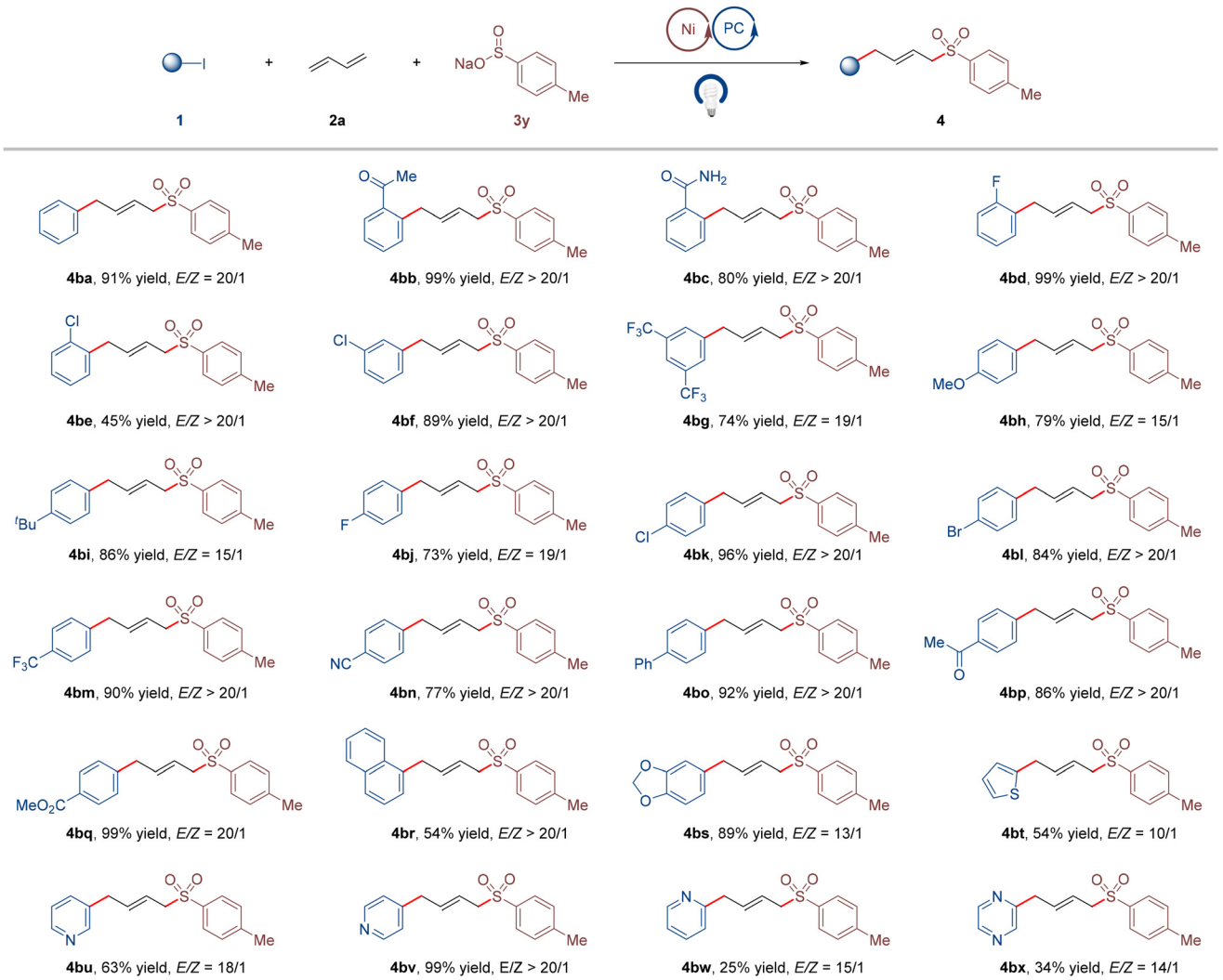

Fig. 3 Substrate scope of (hetero)aryl iodides. Conditions: **1** (0.20 mmol), **2a** (0.60 mmol), **3y** (0.40 mmol), $NiBr_2$·DME (10 mol%), $[Ir(ppy)_2(dtbbpy)]PF_6$ (2 mol%), **L8** (10 mol%), MeCN (1.0 mL), DMSO (0.2 mL), blue LEDs, 24 h, under N_2. Isolated yields are given.

the reaction (Fig. 5a). A radical clock experiment with cyclopropane-substituted styrene **2b** led to the corresponding ring-open product **9**, further indicating the existence of a sulfonyl radical (Fig. 5b). Next, the stereoselectivity of the 1,4-carbosulfonylation product was investigated. No significant isomerization was observed when 1,4-carbosulfonylation product **4aa** was irradiated with different photosensitizers. These results rule out the involvement of photocatalytic *E–Z* isomerization of **4aa**, thus further supporting ligand control of stereoselectivity in the catalytic system (please see the ESI† for details).

To shed light on the nature of the active nickel species in the reaction, several experiments were further carried out. First, the Ar–Ni(II)–I complex ([Ni]-1) was prepared and used in a stoichiometric reaction of butadiene and sodium benzenesulfinate (Fig. 5d). No formation of the corresponding difunctionalized product **4bm** was observed in the reaction mixture (entry 1). However, **4bm** could be detected in 82% yield when using a catalytic amount of [Ni]-1 complex (entry 2), thus, demonstrating the aryl–Ni(II) species as a productive intermediate in this reaction. Next, side product formation in the dual nickel/photoredox-catalyzed carbosulfonylation of butadiene was studied (Fig. 5c). The side product **4aa′** could be observed under an air atmosphere instead of a N_2 atmosphere in a trace amount (entry 4). The yield of **4aa′** was improved slightly when O_2 gas was used (entry 5). The undesired side product **4aa′** probably results from the β-H elimination of allyl nickel species. Afterwards, light on/off control experiments were performed to obtain the reactivity profile of this protocol (Fig. 5e). It was found that the product generation was blocked immediately when the light was turned off and resumed efficiently when turned on. This indicates that constant light irradiation is essential for this transformation. Stern–Volmer experiments were done with iodobenzene **1a**, butadiene **2a**, sodium benzenesulfinate **3a** and $NiBr_2$·DME. These results show that only **3a** could quench the photocatalyst (Fig. 5f and the ESI†).

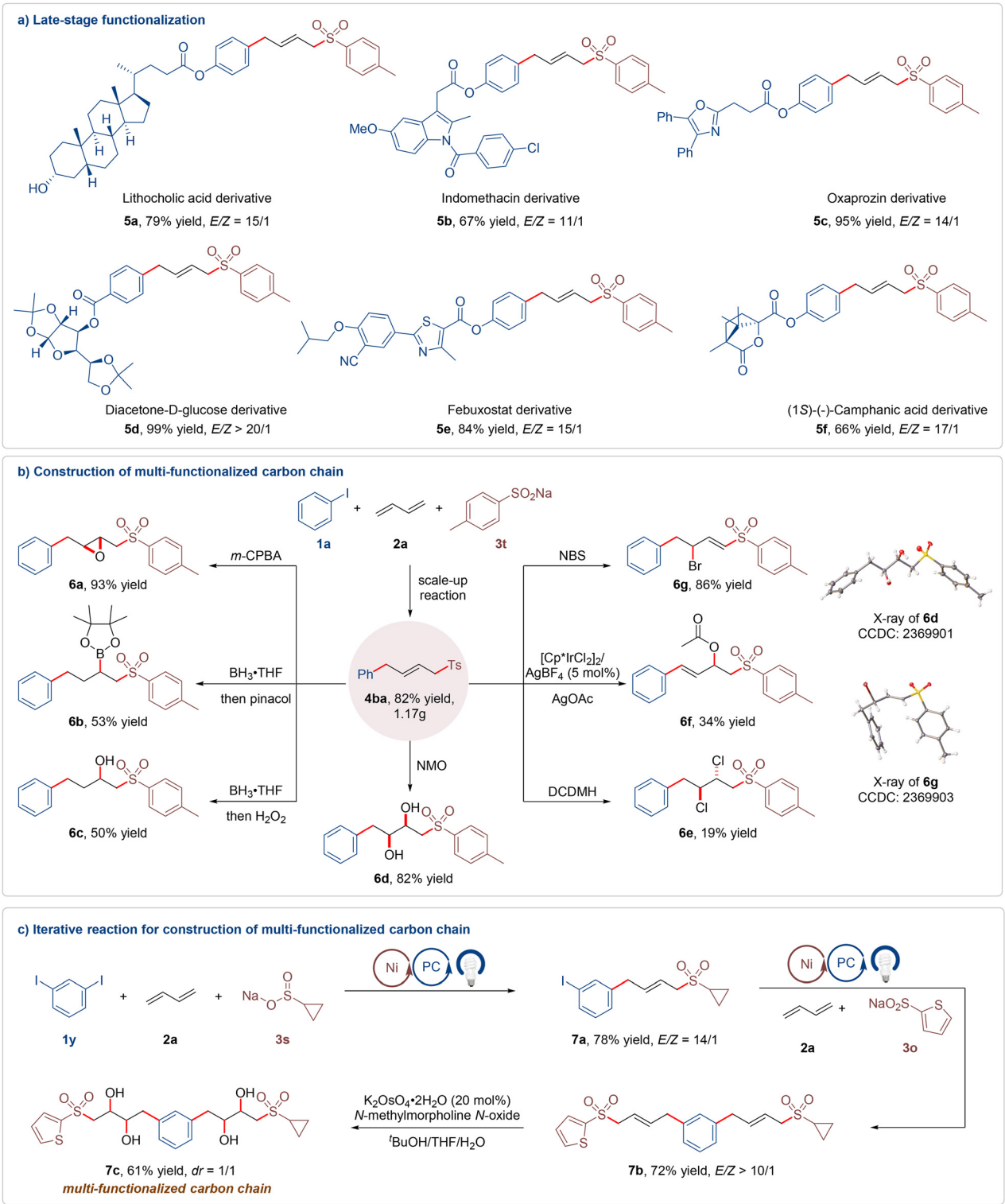

Fig. 4 (a) Late-stage functionalization; (b) construction of multi-functionalized carbon chains; (c) iterative reaction for the construction of multi-functionalized carbon chains.

Based on the above experimental results and literature reports,[13a,f] a plausible mechanism of nickel/photoredox dual catalyzed stereoselective 1,4-carbosulfonylation of butadiene is shown in Fig. 5g. The reaction involves two interconnected catalytic cycles, a photoredox and a cross-coupling cycle. The photoredox cycle starts with the irradiation of $[Ir(ppy)_2(dtbbpy)]PF_6$ with light to enable the excitation of photocatalyst PC*, which oxidizes sodium sulfinate **3** by

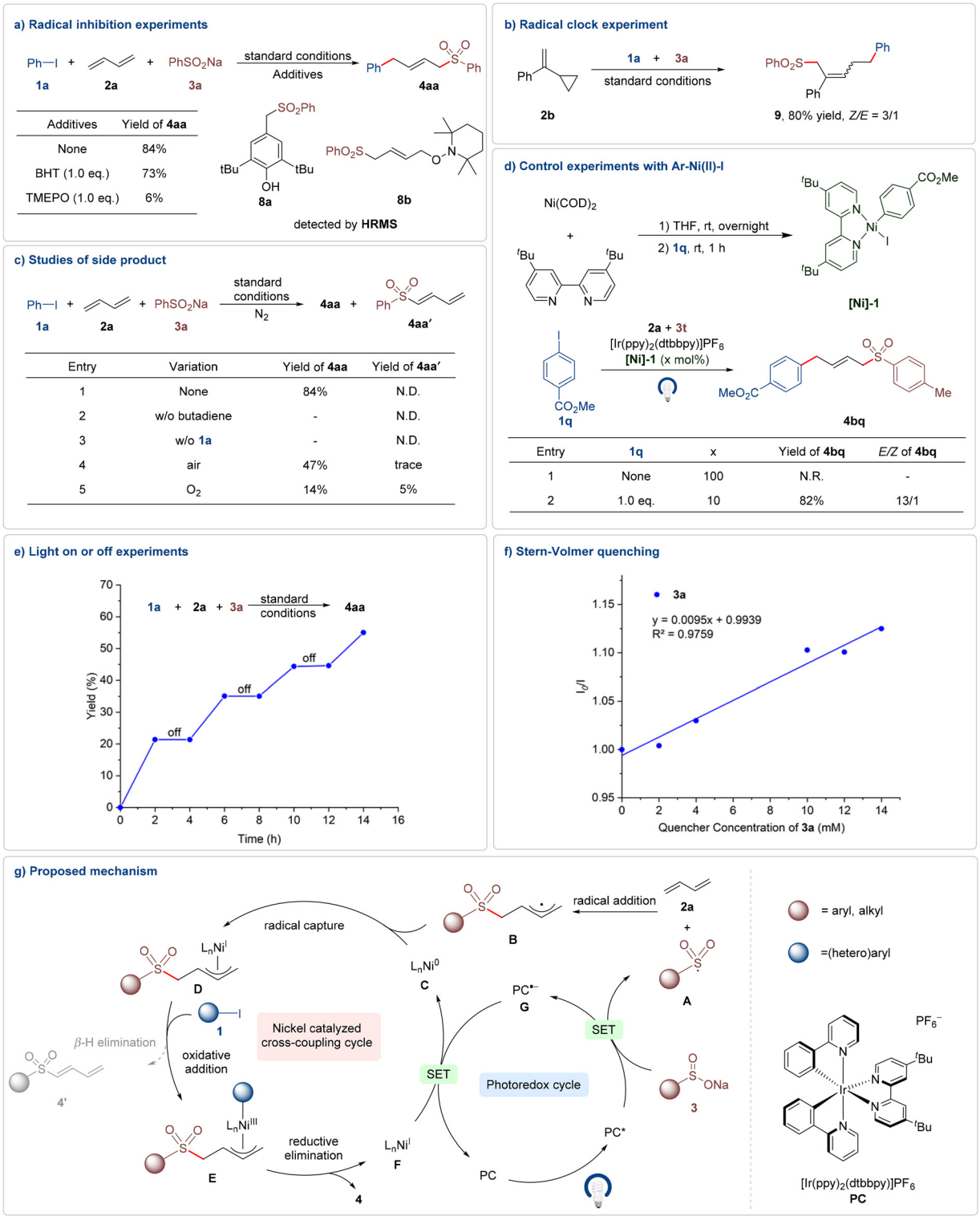

Fig. 5 Mechanistic investigations.

single-electron transfer (SET) to generate the sulfonyl radical **A** and the reduced form of the PC (**G**). The addition of the sulfonyl radical **A** onto butadiene **2a** then produces an allyl radical **B**, which is rapidly captured by Ni(0) species **C** to afford allyl Ni(I) **D**. A subsequent oxidative addition of the aryl iodide **1** to intermediate **D** gives (aryl)(allyl)Ni(III) intermediate **E**. The high-valence Ni(III) intermediate **E** undergoes reductive elimination to furnish the carbosulfonylation product **4** and Ni(I)

species **F**. Finally, single-electron transfer with the reduced form of the PC (**G**) then returns the Ni(I) species **F** to the Ni(0) catalyst **C** and regenerates the ground-state PC. It is worth mentioning that a trace amount of side product **4′** could be observed by the β-H elimination of allyl Ni(I) **D**.

Conclusions

In conclusion, we have developed a photo-induced stereoselective 1,4-carbosulfonylation of butadiene under nickel catalysis to construct multi-functionalized carbon chains. A broad range of aryl iodides and sodium sulfinates were tolerated in this protocol. The derivatives of natural products and pharmaceutically active molecules were proved to be effective reaction partners as well. A range of diverse saturated carbon chains could be created with three, four or more functional groups from butadiene in a unified and concise way. It is hoped that this protocol could provide a complementary approach for the traditional synthesis of multi-functionalized aliphatic compounds.

Data availability

The data supporting this article have been included as part of the ESI.†

Crystallographic data for [**4aa**], [**6d**] and [**6g**] have been deposited at the CCDC under [2335639], [2369901] and [2369903].†

Conflicts of interest

The authors declare no competing financial interest.

Acknowledgements

Financial support from the National Natural Science Foundation of China (22071239 and 22371275) is greatly appreciated.

References

1 (*a*) H.-W. B. Liu and T. P. Begley, *Comprehensive Natural Products III*, 2020; (*b*) K. C. Nicolaou and T. Montagnon, *Molecules That Changed the World*, 2008; (*c*) D. J. Newman and G. M. Cragg, Natural Products as Sources of New Drugs over the Nearly Four Decades from 01/1981 to 09/2019, *J. Nat. Prod.*, 2020, **83**, 770–803; (*d*) Njardarson Group 2022 Small Molecule Top 200, **https://sites.arizona.edu/njardarson-lab/top200-posters/**.

2 B. Desta and G. Amare, Paclobutrazol as a Plant Growth Regulator, *Chem. Biol. Technol. Agric.*, 2021, **8**, 1–15.

3 P. R. Athawale, N. Kumari, M. R. Dandawate, K. Kashinath and D. Srinivasa Reddy, Synthesis of Chiral Tetrahydrofuran Building Blocks from Pantolactones: Application in the Synthesis of Empagliflozin and Amprenavir Analogs, *Eur. J. Org. Chem.*, 2019, 4805–4810.

4 D. Vourloumis, I. Mavridis, A. Athanasoulis, I. Temponeras, D. Koumantou, P. Giastas, A. Mpakali, V. Magrioti, J. Leib, P. van Endert, E. Stratikos and A. Papakyriakou, Discovery of Selective Nanomolar Inhibitors for Insulin-Regulated Aminopeptidase Based on alpha-Hydroxy-beta-amino Acid Derivatives of Bestatin, *J. Med. Chem.*, 2022, **65**, 10098–10117.

5 Y. Elgammal, E. A. Salama and M. N. Seleem, Enhanced Antifungal Activity of Posaconazole Against Candida Auris by HIV Protease Inhibitors, Atazanavir and Saquinavir, *Sci. Rep.*, 2024, **14**, 1571.

6 (*a*) D. A. Colby, R. G. Bergman and J. A. Ellman, Rhodium-Catalyzed C-C Bond Formation via Heteroatom-Directed C-H Bond Activation, *Chem. Rev.*, 2010, **110**, 624–655; (*b*) T. W. Lyons and M. S. Sanford, Palladium-Catalyzed Ligand-Directed C-H Functionalization Reactions, *Chem. Rev.*, 2010, **110**, 1147–1169; (*c*) L. Ackermann, Carboxylate-Assisted Transition-Metal-Catalyzed C-H Bond Functionalizations: Mechanism and Scope, *Chem. Rev.*, 2011, **111**, 1315–1345; (*d*) J. Wencel-Delord, T. Droge, F. Liu and F. Glorius, Towards Mild Metal-Catalyzed C-H Bond Activation, *Chem. Soc. Rev.*, 2011, **40**, 4740–4761; (*e*) S. A. Girard, T. Knauber and C. J. Li, The Cross-Dehydrogenative Coupling of C(sp^3)-H Bonds: A Versatile Strategy for C-C Bond Formations, *Angew. Chem., Int. Ed.*, 2014, **53**, 74–100; (*f*) C. Cheng and J. F. Hartwig, Catalytic Silylation of Unactivated C-H Bonds, *Chem. Rev.*, 2015, **115**, 8946–8975; (*g*) J. He, M. Wasa, K. S. L. Chan, Q. Shao and J. Q. Yu, Palladium-Catalyzed Transformations of Alkyl C-H Bonds, *Chem. Rev.*, 2017, **117**, 8754–8786; (*h*) H. Yi, G. Zhang, H. Wang, Z. Huang, J. Wang, A. K. Singh and A. Lei, Recent Advances in Radical C-H Activation/Radical Cross-Coupling, *Chem. Rev.*, 2017, **117**, 9016–9085; (*i*) P. Gandeepan, T. Muller, D. Zell, G. Cera, S. Warratz and L. Ackermann, 3d Transition Metals for C-H Activation, *Chem. Rev.*, 2019, **119**, 2192–2452; (*j*) Q. Zhao, G. Meng, S. P. Nolan and M. Szostak, N-Heterocyclic Carbene Complexes in C-H Activation Reactions, *Chem. Rev.*, 2020, **120**, 1981–2048.

7 T. Shen and T. H. Lambert, Electrophotocatalytic Diamination of Vicinal C-H Bonds, *Science*, 2021, **371**, 620–626.

8 T. Shen, Y. L. Li, K. Y. Ye and T. H. Lambert, Electrophotocatalytic Oxygenation of Multiple Adjacent C-H Bonds, *Nature*, 2023, **614**, 275–280.

9 (*a*) K. L. Skubi, T. R. Blum and T. P. Yoon, Dual Catalysis Strategies in Photochemical Synthesis, *Chem. Rev.*, 2016, **116**, 10035–10074; (*b*) J. Twilton, C. Le, P. Zhang, M. H. Shaw, R. W. Evans and D. W. C. MacMillan, The Merger of Transition Metal and Photocatalysis, *Nat. Rev.*

Chem., 2017, **1**, 0052; (*c*) A. Y. Chan, I. B. Perry, N. B. Bissonnette, B. F. Buksh, G. A. Edwards, L. I. Frye, O. L. Garry, M. N. Lavagnino, B. X. Li, Y. Liang, E. Mao, A. Millet, J. V. Oakley, N. L. Reed, H. A. Sakai, C. P. Seath and D. W. C. MacMillan, Metallaphotoredox: The Merger of Photoredox and Transition Metal Catalysis, *Chem. Rev.*, 2022, **122**, 1485–1542.

10 (*a*) J. C. Tellis, C. B. Kelly, D. N. Primer, M. Jouffroy, N. R. Patel and G. A. Molander, Single-Electron Transmetalation via Photoredox/Nickel Dual Catalysis: Unlocking a New Paradigm for sp^3-sp^2 Cross-Coupling, *Acc. Chem. Res.*, 2016, **49**, 1429–1439; (*b*) L. Guo, F. Song, S. Zhu, H. Li and L. Chu, syn-Selective Alkylarylation of Terminal Alkynes via the Combination of Photoredox and Nickel Catalysis, *Nat. Commun.*, 2018, **9**, 4543; (*c*) M. W. Campbell, J. S. Compton, C. B. Kelly and G. A. Molander, Three-Component Olefin Dicarbofunctionalization Enabled by Nickel/Photoredox Dual Catalysis, *J. Am. Chem. Soc.*, 2019, **141**, 20069–20078; (*d*) A. Garcia-Dominguez, R. Mondal and C. Nevado, Dual Photoredox/Nickel-Catalyzed Three-Component Carbofunctionalization of Alkenes, *Angew. Chem., Int. Ed.*, 2019, **58**, 12286–12290; (*e*) S. Zhu, X. Zhao, H. Li and L. Chu, Catalytic Three-Component Dicarbofunctionalization Reactions Involving Radical Capture by Nickel, *Chem. Soc. Rev.*, 2021, **50**, 10836–10856.

11 (*a*) R. Romagnoli, P. G. Baraldi, V. Remusat, M. D. Carrion, C. L. Cara, O. Cruz-Lopez, D. Preti, F. Fruttarolo, M. A. Tabrizi, J. Balzarini and E. Hamel, Synthesis and Biological Evaluation of 2-Amino-3-(3′, 4′, 5′-Trimethoxyphenyisulfonyl)-5-Aryl thiophenes as a New Class of Antitubulin Agents, *Med. Chem.*, 2007, **3**, 507–512; (*b*) F. Velazquez, M. Sannigrahi, F. Bennett, R. G. Lovey, A. Arasappan, S. Bogen, L. Nair, S. Venkatraman, M. Blackman, S. Hendrata, Y. Huang, R. Huelgas, P. Pinto, K. C. Cheng, X. Tong, A. T. McPhail and F. G. Njoroge, Cyclic Sulfones as Novel P3-Caps for Hepatitis C Virus NS3/4A (HCV NS3/4A) Protease Inhibitors: Synthesis and Evaluation of Inhibitors with Improved Potency and Pharmacokinetic Profiles, *J. Med. Chem.*, 2010, **53**, 3075–3085.

12 (*a*) D. Q. Dong, Q. Q. Han, S. H. Yang, J. C. Song, N. Li, Z. L. Wang and X. M. Xu, Recent Progress in Sulfonylation via Radical Reaction with Sodium Sulfinates, Sulfinic Acids, Sulfonyl Chlorides or Sulfonyl Hydrazides, *ChemistrySelect*, 2020, **5**, 13103–13134; (*b*) D. Joseph, M. A. Idris, J. Chen and S. Lee, Recent Advances in the Catalytic Synthesis of Arylsulfonyl Compounds, *ACS Catal.*, 2021, **11**, 4169–4204; (*c*) S. Liang, K. Hofman, M. Friedrich, J. Keller and G. Manolikakes, Recent Progress and Emerging Technologies towards a Sustainable Synthesis of Sulfones, *ChemSusChem*, 2021, **14**, 4878–4902; (*d*) X. Ye, X. Wu, S.-r. Guo, D. Huang and X. Sun, Recent Advances of Sodium Sulfinates in Radical Reactions, *Tetrahedron Lett.*, 2021, **81**, 153368; (*e*) J. Corpas, S. H. Kim-Lee, P. Mauleon, R. G. Arrayas and J. C. Carretero, Beyond Classical Sulfone Chemistry: Metal- and Photocatalytic Approaches for C-S Bond Functionalization of Sulfones, *Chem. Soc. Rev.*, 2022, **51**, 6774–6823; (*f*) D. Hu, L. Shen, S. S. H. Chaw, K. Liang and C. Xia, Visible Light-Induced Sulfonylation with Sulfinates as Closed-Shell Radical Acceptors, *Org. Chem. Front.*, 2024, **11**, 3497–3502.

13 (*a*) L. Huang, C. Zhu, L. Yi, H. Yue, R. Kancherla and M. Rueping, Cascade Cross–Coupling of Dienes: Photoredox and Nickel Dual Catalysis, *Angew. Chem., Int. Ed.*, 2020, **59**, 457–464; (*b*) C. Zhu, H. Yue, B. Maity, I. Atodiresei, L. Cavallo and M. Rueping, A Multicomponent Synthesis of Stereodefined Olefins via Nickel Catalysis and Single Electron/Triplet Energy Transfer, *Nat. Catal.*, 2019, **2**, 678–687; (*c*) Y. Chen, K. Zhu, Q. Huang and Y. Lu, Regiodivergent Sulfonylarylation of 1,3-Enynes via Nickel/Photoredox Dual Catalysis, *Chem. Sci.*, 2021, **12**, 13564–13571; (*d*) C. Li, D.-D. Hu, R.-X. Jin, B.-B. Wu, C.-Y. Wang, Z. Ke and X.-S. Wang, Selective 1,4-Arylsulfonation of 1,3-Enynes via Photoredox/Nickel Dual Catalysis, *Org. Chem. Front.*, 2022, **9**, 788–794; (*e*) Z.-L. Liu, Z.-P. Ye, Y.-X. Chen, Y. Zheng, Z.-Z. Xie, J.-P. Guan, J.-A. Xiao, K. Chen, H.-Y. Xiang and H. Yang, Visible-Light-Induced, Palladium-Catalyzed 1,4-Difunctionalization of 1,3-Dienes with Bromodifluoroacetamides, *Org. Lett.*, 2022, **24**, 924–928; (*f*) X. Du, I. Cheng-Sanchez and C. Nevado, Dual Nickel/Photoredox-Catalyzed Asymmetric Carbosulfonylation of Alkenes, *J. Am. Chem. Soc.*, 2023, **145**, 12532–12540; (*g*) T. Long, C. Zhu, L. Li, L. Shao, S. Zhu, M. Rueping and L. Chu, Ligand-Controlled Stereodivergent Alkenylation of Alkynes to Access Functionalized trans- and cis-1,3-Dienes, *Nat. Commun.*, 2023, **14**, 55; (*h*) C. Y. Chang and A. Aponick, Enantioselective Synthesis of Allylic Sulfones via Rhodium-Catalyzed Direct Hydrosulfonylation of Allenes and Alkynes, *J. Am. Chem. Soc.*, 2024, **146**, 16996–17002; (*i*) Z.-L. Liu, Z.-P. Ye, Z.-h. Liao, W.-D. Lu, J.-P. Guan, Z.-Y. Gao, K. Chen, X.-Q. Chen, H.-Y. Xiang and H. Yang, Photoinduced, Palladium-Catalyzed Enantioselective 1,2-Alkylsulfonylation of 1,3-Dienes, *ACS Catal.*, 2024, **14**, 3725–3732; (*j*) T. Zhang, J. Rabeah and S. Das, Red-Light-Mediated Copper-Catalyzed Photoredox Catalysis Promotes Regioselectivity Switch in the Difunctionalization of Alkenes, *Nat. Commun.*, 2024, **15**, 5208.

14 (*a*) S. Y. Guo, F. Yang, T. T. Song, Y. Q. Guan, X. T. Min, D. W. Ji, Y. C. Hu and Q. A. Chen, Photo-Induced Catalytic Halopyridylation of Alkenes, *Nat. Commun.*, 2021, **12**, 6538; (*b*) G.-C. He, T.-T. Song, X.-X. Zhang, Y. Liu, X.-Y. Wang, B. Wan, S.-Y. Guo and Q.-A. Chen, Visible-Light-Induced Catalytic Construction of Tricyclic Aza-Arenes from Halopyridines, *Chem. Catal.*, 2023, **3**, 100793; (*c*) X. X. Zhang, H. Zheng, Y. K. Mei, Y. Liu, Y. Y. Liu, D. W. Ji, B. Wan and Q. A. Chen, Photo-Induced Imino Functionalizations of Alkenes via Intermolecular Charge Transfer, *Chem. Sci.*, 2023, **14**, 11170–11179; (*d*) T. T. Song, Y. K. Mei, Y. Liu, X. Y. Wang, S. Y. Guo, D. W. Ji, B. Wan, W. Yuan and Q. A. Chen, Construction of Bridged

Benzazepines via Photo-Induced Dearomatization, *Angew. Chem., Int. Ed.*, 2024, **63**, e202314304.

15 (*a*) G. Zhang, C.-Y. Zhao, X.-T. Min, Y. Li, X.-X. Zhang, H. Liu, D.-W. Ji, Y.-C. Hu and Q.-A. Chen, Nickel-Catalysed Asymmetric Heteroarylative Cyclotelomerization of Isoprene, *Nat. Catal.*, 2022, **5**, 708–715; (*b*) W. S. Zhang, D. W. Ji, Y. Li, X. X. Zhang, Y. K. Mei, B. Z. Chen and Q. A. Chen, Nickel-Catalyzed Divergent Mizoroki-Heck Reaction of 1,3-Dienes, *Nat. Commun.*, 2023, **14**, 651; (*c*) W. S. Zhang, D. W. Ji, Y. Yang, T. T. Song, G. Zhang, X. Y. Wang and Q. A. Chen, Nucleophilic Aromatization of Monoterpenes from Isoprene under Nickel/Iodine Cascade Catalysis, *Nat. Commun.*, 2023, **14**, 7087.

16 J. Zhang, E. Wang, Y. Zhou, L. Zhang, M. Chen and X. Lin, A Metal-Free Synthesis of 1,1-Diphenylvinylsulfides with Thiols via Thioetherification under Continuous-Flow Conditions, *Org. Chem. Front.*, 2020, **7**, 1490–1494.

17 A. E. Lubaev, M. D. Rathnayake, F. Eze and L. Bayeh-Romero, Catalytic Chemo-, Regio-, Diastereo-, and Enantioselective Bromochlorination of Unsaturated Systems Enabled by Lewis Base-Controlled Chloride Release, *J. Am. Chem. Soc.*, 2022, **144**, 13294–13301.